JOURNAL OF PETROLOGY | VOLUME 39 | NUMBER 11 & 12 | PAGES 1965–1973 | 1998

Complications to Carbonate Melt Mobility due to the Presence of an Immiscible Silicate Melt

WILLIAM G. MINARIK*

GEOPHYSICAL LABORATORY AND DEPARTMENT OF TERRESTRIAL MAGNETISM, CARNEGIE INSTITUTION OF WASHINGTON, 5251 BROAD BRANCH ROAD, WASHINGTON, DC 20015, USA

RECEIVED SEPTEMBER 28, 1997; REVISED TYPESCRIPT ACCEPTED MAY 21, 1998

The relative interfacial energies of immiscible carbonate and silicate melts were investigated in olivine and clinopyroxene matrices. Carbonate melt has a higher melt–solid interfacial energy than does the coexisting silicate melt. The silicate melt therefore selectively wets the grain-edge channels between solid phases, excluding the carbonate melt to the center of melt pockets, away from grain edges. This prevents the carbonate melt from migrating independently of the silicate melt and the carbonate melt is unable to separate from the silicate melt in a solid-dominated assemblage. The carbonate melt will migrate effectively only after the silicate melt has solidified, or by separating from the silicate melt within liquid-dominated reservoirs (sills, dikes, or chambers), unrestricted by solid interfaces. This relative wetting behavior may help explain the close association of carbonate and silicate magmas in alkali complexes, and their relative timing of emplacement. These results also place constraints on the generation and separation of derivative melts in carbonated silicate melt systems and on the style and timing of alkali wall-rock metasomatism.

KEY WORDS: *interfacial energy; carbonate melt; silicate melt; immiscible; wetting*

INTRODUCTION

Carbonatite melts are thought to be ideal metasomatic agents in the crust and upper mantle (Green & Wallace, 1988; Hauri *et al.*, 1993; Rudnick *et al.*, 1993). They are molten at relatively low temperatures, can solvate a number of incompatible elements, and can be very mobile. Their mobility is a result of their low viscosities [0·01–0·1 Pa s at temperatures >500°C, for a range of compositions (Dawson *et al.*, 1990; Wolff, 1994; Dobson *et al.*, 1996)] and their ability to form an interconnected grain-edge melt at low melt fractions. Dunitic assemblages (and probably other mineralogies) with an interconnected carbonate melt should have a high permeability to flow. These melts may transport a variety of trace elements and can infiltrate long distances into the country rock surrounding melt channels, altering the chemistry and isotopic systems of the host rock. Diffusion is fast within these melts, so even a stagnant interconnected melt can greatly enhance the transport of trace and major elements (Watson, 1991).

The relative interfacial energy between grain–grain contacts and grain–fluid contacts can be parameterized by the dihedral angle, the angle subtended at a fluid–grain–grain junction. Dihedral angles >60° indicate that system interfacial energy is minimized by reducing the contact of the fluid with the solid, whereas systems with dihedral angles <60° minimize interfacial energy by spreading the fluid out along grain-edge tubes (termed a wetting fluid). A low-abundance fluid does not spread across the faces of the mineral grains unless the dihedral angle is zero, which is not generally the case for mantle fluids. Of mantle fluids, carbonate melts have some of the lowest interfacial energies with respect to mantle minerals. Dihedral angles are in the range of 25–30° in contact with olivine, and depend only weakly on melt composition, temperature, or pressure (Hunter & McKenzie, 1989; Watson *et al.*, 1990). Dihedral angles

*Telephone: (202) 686-2410. Fax: (202) 686-2419.
e-mail: minarik@gl.ciw.edu

of carbonate melts in contact with other minerals have not been determined, but presumably are low for many silicates (cpx <60°, Brenan & Watson, 1991). These very low dihedral angles imply that carbonate melts will form an interconnected grain-edge network at very low melt fractions.

Dihedral angle theory assumes a single fluid in contact with a single solid phase which has an isotropic interfacial energy. Most minerals have interfacial energy that varies with crystallographic orientation, to greater or lesser extent. In cases of minerals with certain high-energy crystallographic orientations (a function of the atomic composition of the surface and the surface-active components of the fluid), the mineral will form flat planes (facets) that are oriented to minimize the grain's interfacial energy, especially at large fluid fractions. These facets are distinct from the planes formed perpendicular to fast-growth directions (growth facets) and represent a stable morphology of the mineral grain. Facets complicate the determination of interconnectivity, as the dihedral angle can be measured only on curved interfaces and the facets disturb the idealized geometry of the grain-edge fluid network (e.g. Faul, 1997). Olivine has some interfacial energy anisotropy but shows a limited tendency to facet (Cooper & Kohlstedt, 1982), whereas clinopyroxene frequently forms facets (Watson & Lupulescu, 1993).

Although theory predicts interconnectivity for melts with dihedral angles <60° at all melt fractions, transport experiments have shown that there exists a finite melt fraction below which the melt is not interconnected. Solid phases with high solid–melt interfacial energies and interfacial energy anisotropy will promote melt-free grain edges, resulting in loss of interconnectivity. The onset of interconnectivity has been estimated to occur at <0·05 vol. % melt for millimeter-sized mantle assemblages, based on experiments using a fine-grained olivine matrix and sodium carbonate melt (Minarik & Watson, 1995). On the other hand, deformation of the assemblage will probably promote interconnectivity and melt mobility (Daines & Kohlstedt, 1997).

The presence of a second, immiscible fluid (such as a CO_2-rich vapor or a conjugate silicate melt) will give rise to more complicated behavior, and can inhibit the migration of the fluid at low fluid fractions. For example, the presence of an interval of coexisting H_2O–CO_2 vapor and fluid has been proposed as a mechanism for trapping migrating fluids in the mid-crust (Bailey, 1994). The migration and extraction of two-phase fluids has been extensively studied in the oil literature (e.g. Alder & Brenner, 1988), but igneous systems differ from shallow aquifers in that textural equilibration between fluid and solid controls the size and shape of the pores and of the grain-edge channels connecting them. The resulting microstructure and permeability of the system are the result of the interplay between competing interfacial energies and depend on pressure, temperature, phase compositions, and fluid abundance.

The generation of carbonatite melts from a carbonated silicate melt through immiscibility has been proposed as an explanation for the occurrence of paired carbonatite–silicate magmatic centers, and has been extensively investigated experimentally. Lee & Wyllie (1997*a*, 1997*b*, 1998) have reviewed the experimental and geologic evidence for carbonatite–silicate immiscibility. These experimental studies suggest that it is unlikely that primary carbonate or carbonated silicate mantle melts will intersect the field of immiscible melt stability, but that evolved mantle-derived carbonated silicate melts within the crust may exsolve a carbonate melt, especially in more alkali-rich systems (Baker & Wyllie, 1990; Kjarsgaard & Peterson, 1991; Kjarsgaard *et al.*, 1995).

Strong evidence for naturally occurring immiscible melts in the crust has been described at Oldoinyo Lengai (Dawson *et al.*, 1994; Church & Jones, 1995; Dawson *et al.*, 1996), Suswa (MacDonald *et al.*, 1993), and Shombole (Kjarsgaard & Peterson, 1991) volcanoes in the East African Rift system. These extrusives contain carbonate-rich spheres (ocelli) within the silicate matrix or silicate spheres (Oldoinyo Lengai) within a carbonate matrix. Further examples of proposed crustal carbonate–silicate immiscibility are the Dolbykha complex in Siberia (Kogarko, 1997) and the Italian carbonatites (Stoppa & Woolley, 1997). The compositions of the carbonate ocelli have been modified by subsequent recrystallization and fluid transport, but in some cases are comparable with those of experimentally determined melt pairs (Lee *et al.*, 1994; Lee & Wyllie, 1998).

Mafic silicate melts have low dihedral angles (20–50°, Holness, 1997) in contact with olivine and other silicate minerals. This range is generally higher than the dihedral angles for carbonate melts, but the ranges overlap. Silicate melts are not thought to be as mobile as carbonate melts nor as effective at metasomatism because of their higher viscosities (10–10^3 Pa s) (McKenzie, 1985). It was not clear from previous results what would be the distribution of coexisting immiscible silicate and carbonate melts in a silicate matrix. The presence of two melts should have consequences for the mobility of these melts, and these consequences would depend on whether the silicate melt or carbonate melt filled the grain-edge channels.

In this study reconnaissance experiments were performed to investigate the microstructure of immiscible melts and the implications for transport and separation of these melts. The results show that where conjugate silicate and carbonatite melts are present within a dunitic or wehrlitic matrix, the silicate melt preferentially fills the grain-edge channels and isolates the carbonate melt pods from one another. This microstructure significantly inhibits the mobility of the carbonate melt and reduces its ability to act as an ephemeral metasomatic agent.

EXPERIMENTAL AND ANALYTIC METHODS

Mafic melts with several different alkali contents were chosen that would generate melt pockets large enough to produce clearly immiscible melts, but still small enough to interact with the surfaces of a large number of mineral grains. Although large melt fractions were used to elucidate the relative wetting behavior of these melts, the results of these experiments are applicable to low-abundance melts. Carbonated silicate melts and carbonate melts are both notoriously difficult to quench isochemically, especially when in contact with mineral surfaces, so these experiments are not optimal for the determination of the compositions of the coexisting immiscible melts. A pressure of 1·5 GPa was chosen as a compromise that would combine a relatively large immiscible region (immiscibility decreases with increasing pressure) with the potential to stabilize relatively alkali-poor carbonate melts (which react at low pressures). Olivine was chosen as the matrix, because of the large literature on olivine–melt microstructure and because it is the dominant mineral of the upper mantle. The microstructure of a clinopyroxene matrix was also investigated, as natural mantle dolomitic carbonatitic melts will react with peridotite at pressures below 1·5–2·0 GPa to produce clinopyroxene and CO_2 (Dalton & Wood, 1993).

Compositions of the starting materials and the proportions of these materials used in the experimental charges are given in Tables 1 and 2 and plotted in Fig. 1. Finely powdered (<38 μm) carbonate, basaltic glass, and mineral (either olivine or clinopyroxene) were mixed to give bulk compositions that contained melt plus ~60–70 vol. % solid at the run conditions. Mixes 1, 3, and 4 fall within the immiscible melt volume at 1·5 GPa, whereas Mix 2 lies within the single melt region. All the experiments but one contain olivine as the solid matrix phase (the exception is Experiment PC 243 which contains clinopyroxene). The mixes were dried at 200°C overnight and stored at 110°C to minimize the amount of adsorbed water.

These starting mixtures were contained within graphite-lined platinum capsules, sealed by welding, and placed within standard GL 3/4 inch (19 mm) tapered-furnace talc–Pyrex®–AlSiMag® piston-cylinder assemblies (Boyd & England, 1960; Kushiro, 1976). The piston-in technique with a –7·5% friction correction was used, and temperature was controlled with W5%Re/W26%Re thermocouples with no correction to the e.m.f. for pressure. The iron-bearing starting materials were pre-equilibrated at the 1 atm quartz–fayalite–magnetite buffer before use, and the oxygen fugacity during the experiments is just below that of the graphite–CO_2 buffer. All of the experiments except one were taken to the run pressure and then directly heated to the run temperature.

Table 1: Starting material compositions (in wt %)

	Olivine	Clinopyroxene	Kilauea Iki basalt
SiO_2	40·84	53·04	46·80
TiO_2	0·01	0·15	2·02
Al_2O_3	0·03	3·42	9·55
FeO*	9·18	2·5	11·75
MnO	0·14	0·12	0·16
MgO	49·65	17·08	17·64
CaO	0·09	21·69	8·57
NiO	0·41	n.d.	0·11
Na_2O	n.d.	0·85	1·56
K_2O	n.d.	n.d.	0·40
P_2O_5	n.d.	n.d.	0·19
Cr_2O_3	0·04	1·23	0·16
Total	100·39	100·08	98·91

San Carlos olivine and clinopyroxene compositions from Brenan & Watson (1991), Kilauea Iki basalt composition determined using ICP by Stan Mertzman, Franklin & Marshall College and accurate to within 1% relative (Boyd & Mertzman, 1987). FeO* is total iron; n.d., not determined.

Table 2: Proportions (wt %) of starting materials

	Mix 1	Mix 2	Mix 3	Mix 4
Na_2CO_3	18·38	2·36	12·77	20·48
$MgCa(CO_3)_2$	—	13·55	4·74	—
Olivine	61·82	69·56	64·53	—
Clinopyroxene	—	—	—	59·59
Basalt	19·80	14·53	17·96	19·93

Experiment PC 237 was first heated to 1400°C (above the solvus) for 24 h before the temperature was reduced to the run temperature of 1150°C at 10°/min. Experimental microstructures were preserved at the end of the runs by cutting power to the furnace, resulting in a quench rate of greater than 200°C/s.

Samples were mounted in epoxy and polished using oil-based diamond paste. Kerosene was used as a lubricant and cleaner to prevent dissolution of the carbonate. The samples were carbon-coated and a JEOL 8900 electron microprobe was used to obtain backscattered images, X-ray maps and quantitative concentrations. Low currents (5–10 nA) and a 10–20 μm rastered beam were used to minimize sodium loss; under these conditions sodium X-ray count rates remain constant over the course

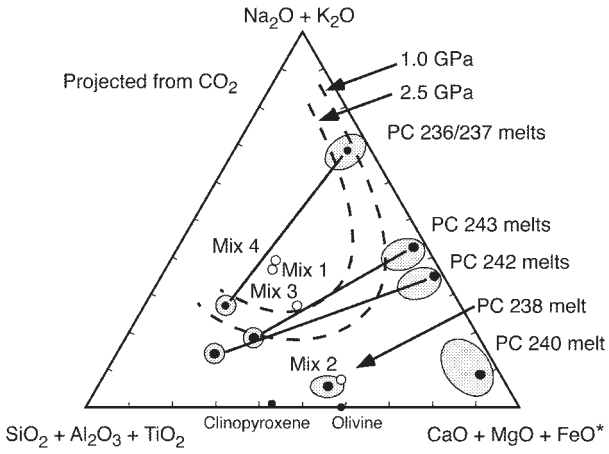

Fig. 1. Starting carbonate + basalt compositions without the matrix mineral (○, Mixes 1–4) plotted on the modified ternary Hamilton projection from CO_2 (Freestone & Hamilton, 1980). ●, average analyzed compositions, joined by a bold tie-line in the case of immiscible melts. These averages are surrounded by a dotted region that encompasses the majority of the individual melt determinations. Dotted lines indicate the immiscibility limits at 1 and 2·5 GPa after Lee & Wyllie (1997*a*) and Baker & Wyllie (1990).

contained two immiscible melts; the carbonate melt forming rounded blebs surrounded by the silicate melt and separated by a smooth meniscus.

In each experiment the silicate melts wet the olivine and clinopyroxene matrix—these melts are in contact with the grains, fill the grain-edge channels, and form an interconnected grain-edge network (Fig. 2). The distribution of each of the silicate melts is consistent with a dihedral angle of <60°, as reported for other mafic silicate melts in contact with olivine [summarized by Holness (1997)]. These angles were not measured for these experiments, in part because of the crystal faceting of both olivine and clinopyroxene. Single carbonated silicate melts (e.g. PC 238 and 240) would remain interconnected at much lower melt fractions, forming a fast pathway along grain edges for chemical diffusion, and allowing migration of this melt from its source area. Such a single carbonated silicate melt may be similar to natural melts that are capable of precipitating both carbonate and silicate minerals.

The other experiments produced two immiscible melts, and in each case the carbonate melt was isolated from contact with the grain boundaries by the silicate melt.

Table 3: Experimental conditions

Experiment	*T* (°C)	*P* (GPa)	Time (h)	Composition (matrix)	Resulting phases
PC 236	1150	1·5	67·3	Mix 1 (Olivine)	Two melts, olivine
PC 237	1150	1·5	121·6	Mix 1 (Olivine)	Two melts, olivine
PC 238	1150	1·5	53·3	Mix 2 (Olivine)	One melt, olivine
PC 240	1100	1·5	100·4	Mix 2 (Olivine)	One melt, olivine, cpx
PC 242	1150	1·5	34·1	Mix 3 (Olivine)	Two melts, olivine
PC 243	1150	1·5	35·7	Mix 4 (Clinopyroxene)	Two melts, cpx, olivine

of the analysis. Olivine or pyroxene standards were used for the mineral analyses, and a basalt standard was used for the silicate and carbonate melt analyses with CO_2 determined by difference and X-ray intensities corrected using the ZAF scheme. Average melt compositions were estimated by combining several rastered analyses from random locations within the heterogeneous quenched melt pockets.

RESULTS

The experimental run conditions are given in Table 3. The experiments resulted in quenched melt dispersed within a matrix of olivine (PC 236–PC 242) or clinopyroxene (PC 243). The melt remained distributed throughout the capsule, without gravitational segregation. The two runs using the low-alkali mixture (Mix 2) contained only one quenched melt, whereas the other runs Separately, each melt would have a dihedral angle <60° and would wet the grain edges, but with coexisting melts only the lowest interfacial energy melt (the silicate melt) contacts the solid grains. This is true for experiments containing olivine and clinopyroxene matrices, and similar textures were generated when the experiment was brought directly to run conditions (PC 236) or cooled from above the solvus (PC 237), demonstrating that the melt distribution was independent of the initial distribution. In some experiments (Fig. 2), smaller carbonate melt pockets have coalesced to form larger pockets surrounded by multiple grains, all coated with silicate melt.

During the experiments, the grain size increased from the initial <38 μm to an average of 50 μm diameter (range of 10–70 μm). The largest olivines have compositionally zoned cores, as the run durations were not sufficient for lattice diffusion to homogenize all the grains. The boundaries of the grains recrystallized rapidly, and the

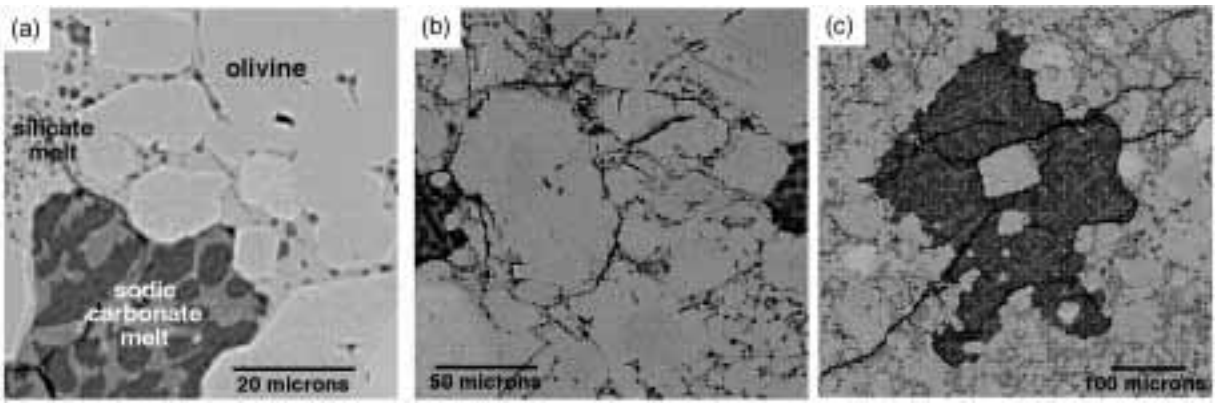

Fig. 2. Backscattered electron maps of experiment PC 236. Silicate melt (light gray) preferentially fills the grain-edge channels and relegates the carbonate melt (dark gray) to isolated melt pockets. These pockets can communicate only via diffusion through the silicate melt. The carbonate melt has quenched to a matte of calcite, alkali carbonate, and silicate.

Table 4: Estimated melt compositions; CO_2 determined by difference

	PC 236/PC 237		PC 238	PC 240	PC 242		PC 243	
	Carbonate	Silicate	One melt	One melt	Carbonate	Silicate	Carbonate	Silicate
SiO_2	03·0	37·6	23·5	0·8	1·4	41·7	1·9	38·7
TiO_2	0·3	1·6	1·4	0·2	0·1	2·0	0·0	0·6
Al_2O_3	0·2	9·0	7·3	2·1	0·2	11·5	0·4	6·2
FeO*	2·5	6·1	8·0	2·5	1·8	5·7	1·3	5·1
MgO	5·9	7·4	8·9	9·3	5·3	6·0	6·8	9·8
CaO	7·2	3·3	24·5	41·2	34·9	8·4	25·9	10·9
Na_2O	40·1	23·3	3·9	4·6	22·7	11·9	25·8	15·6
CO_2	40·4	11·4	22·0	38·7	33·3	12·3	37·6	12·9

run products have the smoothly curving interfaces characteristic of textural equilibrium. Some faceting of olivine was observed on the faces bordering melt pockets, and considerable faceting was evident in the clinopyroxene. Faceting is a manifestation of interfacial energy anisotropy, and illustrates one limitation of dihedral angle theory.

None of the melts quenched to a glass; during the several-second temperature quench the melts continued to unmix until they reached solidus. Additionally, the melts have plated out quench rims on the matrix minerals and precipitated quench minerals (including calcite dendrites in the carbonate quenched melt). These quench modifications make determination of the composition of the melts during the run difficult; more accurate melt compositions would require a different experimental design. Estimates of paired melt compositions determined by averages of large-area rastered electron beam analyses are included in Table 4. The analyses show considerable scatter and have not been corrected for material plated onto the rims of the matrix minerals. As such they are provided for reference only and should not be used as actual melt compositions. These compositions and an indication of the scatter of analysis are plotted in Fig. 1, referenced to the immiscibility gaps determined at 1·0 and 2·5 GPa. Concentration maps for Si, Na and Ca are shown in Fig. 3; the melts are clearly delineated from one another, with the carbonate melt enriched in sodium and calcium and the silicate melt enriched in aluminum, iron, magnesium and titanium. Both melts contain all components, however.

The compositions of the matrix minerals have adjusted to be in equilibrium with the melt; the rims of the matrix olivine have gained iron (to 9·7 wt % FeO from 9·5 wt % FeO initially) and the clinopyroxenes of PC 243 have lost iron and aluminum and gained calcium and sodium from the initial San Carlos composition. The adjustments are subtle and the new mineral compositions would plot on top of the initial compositions on the scale of Fig. 1. Two of the experiments contained additional stable

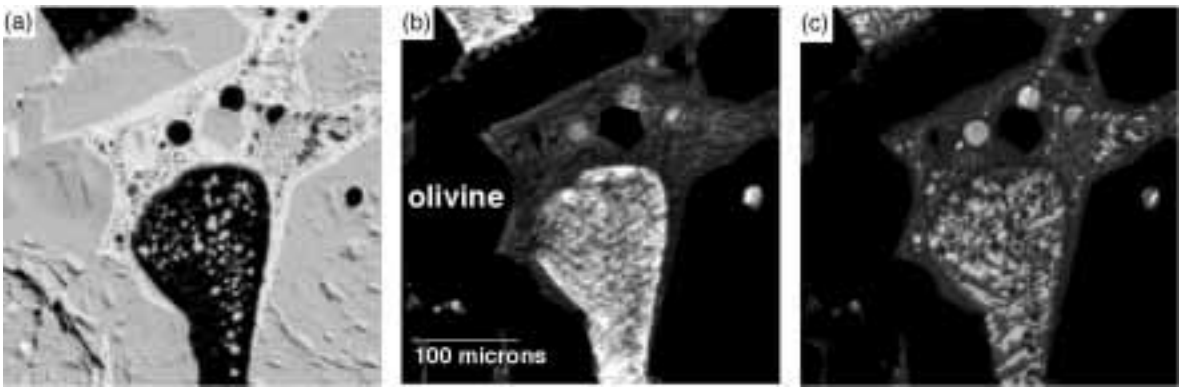

Fig. 3. X-ray intensity maps of experiment PC 237, for (a) Si, (b) Na, and (c) Ca. Brighter areas indicate higher concentration of the element mapped. The carbonate melt is isolated from contact with the olivine by the silicate melt. Both melts have unmixed further on quench, filling each quenched melt with small spheres of the conjugate melt and quench crystals. There is also a several micron thick quench rind on the matrix olivine. The silicate material within the carbonate melt represents silicate dissolved within the melt at the run conditions. The maps are 400 × 400 pixel images, with 100 ms dwell per pixel at 60 nA cup current.

phases (Table 3). The 1100°C PC 240 crystallized clinopyroxene (accounting for the shift in melt composition), and PC 243 contains a few scattered olivine crystals, probably as the result of contamination in the initial clinopyroxene separate.

DISCUSSION

In these systems the silicate melt has a lower mineral–melt interfacial energy than does the carbonate melt. As the interfacial energy of carbonate melts in contact with olivine does not vary with composition (Watson *et al.*, 1990), it implies that the addition of alkalis and carbonate to mafic magmas reduces their interfacial energy to the lower end of the measured range. The structure of silicate melts at the crystal interface is largely unknown, as is the identity of surface active species (Wanamaker & Kohlstedt, 1991). Examination of fig. 4a (Exp. L71) of Lee & Wyllie (1997*b*) suggests that olivine is also wetted by a nephelinic melt in preference to a carbonate melt at 2·0 GPa and 1225°C. The same relative interfacial energies apply to clinopyroxene in the current study.

A natural example may provide relative wetting information for other minerals and conditions. Stoppa & Woolley (1997) described lapilli tuffs of the Italian carbonatite locality Monticchio. These mixed carbonatite–melilitite deposits contain mantle xenocrysts and may be the result of a carbonated magma that evolved an immiscible carbonate melt at low pressure as it rapidly ascended. The lapilli consist of cores of amphibole, clinopyroxene and olivine surrounded by a shell of melilitite surrounded by a shell of carbonatite. If these lapilli represent immiscible melts, and if the texture represents a interfacial energy-determined structure (instead of an accident of fragmentary eruption), then this silicate melt preferentially wets these silicates at crustal pressures. Clearly, more experiments need to be carried out at crustal pressures and assemblages.

Silicate melt preferentially occupies the grain-edge channels in these immiscible systems, forcing chemical communication between isolated pockets of the carbonate melt to take place only via diffusion through the intervening silicate melt (Fig. 2b). The presence of immiscible fluid (the carbonate melt) bubbles will provide resistance against the bulk migration of the two-phase fluid (or of the silicate melt alone) by 'plugging' access to grain-edge channels (Fig. 4). The carbonatitic–silicate melt interface curvature will increase as the carbonate melt bubble is forced into the throat of the channel, and this interface curvature results in an opposing pressure to flow (Bailey, 1994). This resistance to flow may allow larger melt fractions to accumulate before they eventually migrate via fractures or dikes.

In a static system, a stable mineral is in equilibrium compositionally with both conjugate silicate and carbonate melts; the bulk chemical potentials are equal for both melts and crystal. In this case, the composition of the mineral will be the same whether the carbonate melt or the silicate melt is in contact with it. In dynamic systems, where minerals are growing fast relative to diffusive homogenization of the melt compositions, a growing mineral could deplete the silicate melt in contact with it of those elements preferentially partitioned into the carbonate melt (i.e. light rare earth elements and large ion lithophile elements; Jones *et al.*, 1995). Such mineral zoning might record the onset of immiscibility in an evolving magmatic system.

Pyle & Haggerty (1994) described four metasomatized eclogitic xenoliths from the Jagersfontein kimberlite in South Africa. Two eclogites are pervasively metasomatized, whereas two contain metasomatic minerals

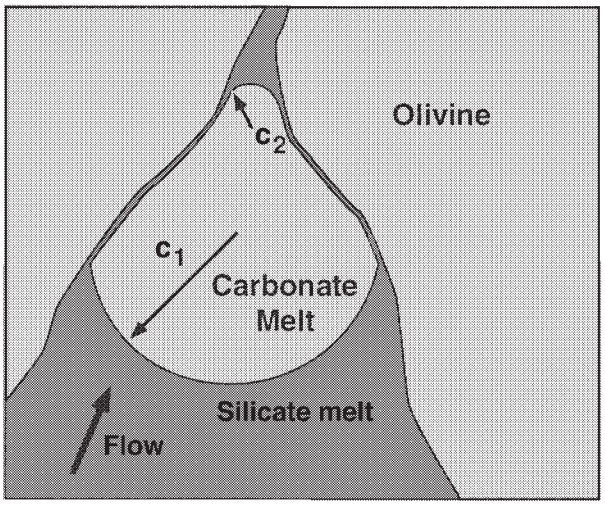

Fig. 4. A schematic diagram of two immiscible melts flowing in a grain-edge channel after Bailey (1994). Flow of the carbonate melt is inhibited by the increase in mean curvature of the carbonate–silicate melt interface (radius c_1 to c_2) as the carbonate melt enters the channel. This interfacial tension will counteract the flow. The carbonate melt, in turn, restricts the movement of the silicate melt by plugging the grain-edge channel.

(carbonate, natrolite, barite, and pectolite) only in veins. These veined xenoliths contain calcium carbonate- and hydrous-Na–Al silicate-rich ocelli surrounded by silicate glass, which Pyle & Haggerty took as evidence for the presence of immiscible carbonate and silicate melts. If these ocelli do represent the presence of immiscible melts, then the association between immiscible melts and metasomatic alteration products restricted to veins may be explained by the differing mobilities of single and two liquid phase systems described above. A single carbonated silicate melt migrating into an eclogitic assemblage would have a dihedral angle <60° and would pervasively wet the grain-edge channels. On the other hand, if this melt unmixed into immiscible silicate and carbonate melts, its mobility would be restricted by the presence of the non-wetting carbonate melt pockets. The silicate melt would not flow as easily along the grain-edge channels because of the plugging effect of carbonate melt, and much of the carbonate and alkalis would remain within the original veins. The ocelli have undoubtedly been modified subsequent to crystallization, and reconstructed conjugate melt compositions are not close to the experimental immiscibility gap (Lee & Wyllie, 1998). It may be that these ocelli and rounded calcite represent carbonate and silicate minerals co-precipitated from a single melt, or from sequential fluids. The model of Pyle & Haggerty requires the injection of a CO_2-rich fluid into a partially molten precursor, which may be mechanically difficult.

By analogy, the behavior described above for two-melt systems also applies to systems containing melt and vapor. Silicate or carbonatitic melt evolving a CO_2-rich vapor [such as shown by Yaxley & Green (1996)] would develop isolated vapor pockets surrounded by melt-filled grain-edge channels. These pockets would be unable to separate from the melt until the melt fraction was large enough to allow the phases to separate without squeezing through grain-edge constrictions. Retention of the vapor would greatly increase the buoyancy of the fluid system, and contribute to fracturing and rapid eruption once the vapor started exsolving. Conversely, introduction of an H_2O–CO_2 fluid into a partially molten system would be unlikely. The fluid could not readily displace the melt from grain-edge channels. Injection by fracturing a partially molten matrix might allow H_2O–CO_2 fluid introduction; the fluid veins would break up, and then would heal into isolated fluid pockets surrounded by melt-filled channels.

Primary carbonate melts rising through the mantle may not often collect into melt-dominated reservoirs, as their low viscosity and low dihedral angle let them leak away along grain-edge channels. Melts that react with peridotite and evolve CO_2 may do so fast enough to fracture a channel and form high-permeability pathways to the surface that allow transient maar eruptions. Evolution of immiscible melts, however, can facilitate the formation of carbonatite-rich intrusions and reservoirs. The relative interfacial energies of immiscible melts may account for the close association of carbonatites and silicate magmas in eruptive centers; the immiscible melts would be unable to effectively separate until they reached a liquid-dominated volume (a sill, dike or chamber). Once the melts have collected into larger volumes, their segregation will be unimpeded by the grain-edge channel constrictions and they can gravitationally separate. The silicate melt will still seal the margins of the chamber; removal of the melt would require fracturing of the wall rock. If immiscibility is generally reached late in the fractionation of a carbonated silicate melt, then this carbonate melt would be confined to the center of the complex, and may erupt only after the silicate melt has solidified. This provides one explanation for the observation that the carbonate melt always erupts last in carbonate–silicate alkali complexes (Bailey, 1993).

This mechanism suggests that loss of alkalis to the country rock via a carbonate melt and the resulting fenitization is inefficient after the evolution of immiscible carbonate and silicate melts. Similarly, the loss of a CO_2–H_2O vapor will be inhibited by the presence of a coexisting silicate melt. The expulsion of an alkali-rich carbonate melt or vapor as a pervasive metasomatic agent will resume only after the solidification of the silicate melt. The restricted mobility of an alkali-rich fluid phase probably enhances sub-solidus recrystallization, which may erase the textural evidence for immiscibility (the extent of compositional rearrangement during

quench of these experiments suggests the magnitude of the problem in interpreting natural systems).

CONCLUSIONS

Preliminary experiments examining the microstructure of immiscible silicate and carbonate melts in a polycrystalline matrix demonstrate that the silicate melt preferentially wets the silicate matrix. This implies that carbonate melt mobility is severely restricted while the melt is present in small grain-edge channels. Effective separation of silicate from the carbonate melts requires larger crystal-poor volumes, overpressuring to cause fracturing, or solidification of the silicate melt. This restricted carbonate melt mobility in a two-melt system is in contrast to the expected high mobility of a isolated carbonatite melt. Models of carbonatite formation and evolution need to be consistent with the physical microstructural constraints as well as the chemical and isotopic constraints.

ACKNOWLEDGEMENTS

Bjørn Mysen kindly provided access to the piston-cylinder apparatus. Discussions with James Brenan, Nathalie Marchildon, Rick Ryerson and Bruce Watson improved this study, as did formal reviews by Harry Pinkerton, David Pyle, John Dalton and Keith Bell.

REFERENCES

Alder, P. M. & Brenner, H. (1988). Multiphase flow in porous media. *Annual Review of Fluid Mechanics* **20,** 35–59.

Bailey, D. K. (1993). Carbonate magmas. *Journal of the Geological Society, London* **150,** 637–651.

Bailey, R. C. (1994). Fluid trapping in mid-crustal reservoirs by H_2O–CO_2 mixtures. *Nature* **371,** 238–240.

Baker, M. B. & Wyllie, P. J. (1990). Liquid immiscibility in a nephelinite–carbonate system at 25 kbar and implications for carbonatite origin. *Nature* **346,** 168–170.

Boyd, F. R. & England, J. L. (1960). Apparatus for phase-equilibrium measurements at pressures up to 50 kilobars and temperatures to 1750°C. *Journal of Geophysical Research* **65,** 741–748.

Boyd, F. R. & Mertzman, S. A. (1987). Composition of structure of the Kaapvaal lithosphere, southern Africa. In: Yoder, H. S. & Mysen, B. O. (eds) *Magmatic Processes: Physicochemical Principles*. University Park, PA: Geochemical Society, pp. 13–24.

Brenan, J. M. & Watson, E. B. (1991). Partitioning of trace elements between carbonate melt and clinopyroxene and olivine at mantle *P–T* conditions. *Geochimica et Cosmochimica Acta* **55,** 2203–2214.

Church, A. A. & Jones, A. P. (1995). Silicate–carbonate immiscibility at Oldoinyo Lengai. *Journal of Petrology* **36,** 869–889.

Cooper, R. F. & Kohlstedt, D. L. (1982). Interfacial energies in the olivine–basalt system. In: Akimoto, S. & Manghnani, M. H. (eds) *High Pressure Research in Geophysics*. Tokyo: Center for Academic Publications, pp. 217–228.

Daines, M. & Kohlstedt, D. (1997). Influence of deformation on melt topology in peridotites. *Journal of Geophysical Research—Solid Earth* **102,** 10257–10271.

Dalton, J. A. & Wood, B. J. (1993). The compositions of primary carbonate melts and their evolution through wallrock reaction in the mantle. *Earth and Planetary Science Letters* **119,** 511–525.

Dawson, J. B., Pinkerton, H., Norton, G. E. & Pyle, D. M. (1990). Physicochemical properties of alkali carbonatite lavas: data from the 1988 eruption of Oldoinyo Lengai, Tanzania. *Geology* **18,** 260–263.

Dawson, J. B., Pinkerton, H., Pyle, D. M. & Nyamweru, C. (1994). June 1993 eruption of Oldoinyo Lengai, Tanzania: exceptionally viscous and large carbonatite lava flows and evidence for coexisting silicate and carbonate magmas. *Geology* **22,** 799–802.

Dawson, J. B., Pyle, D. M. & Pinkerton, H. (1996). Evolution of natrocarbonatite from a wollastonite nephelinite parent: evidence from the June 1993 eruption of Oldoinyo Lengai, Tanzania. *Journal of Geology* **104,** 41–54.

Dobson, D. P., Jones, A. P., Rabe, R., Sekine, T., Kurita, K., Taniguchi, T., Kondo, T., Kato, T., Shimomura, O. & Urakawa, S. (1996). *In-situ* measurement of viscosity and density of carbonate melts at high pressure. *Earth and Planetary Science Letters* **143,** 207–215.

Faul, U. H. (1997). Permeability of partially molten upper mantle rocks from experiments and percolation theory. *Journal of Geophysical Research—Solid Earth and Planets* **102,** 10299–10311.

Freestone, I. C. & Hamilton, D. L. (1980). The role of liquid immiscibility in the genesis of carbonatites—an experimental study. *Contributions to Mineralogy and Petrology* **73,** 105–117.

Green, D. H. & Wallace, M. E. (1988). Mantle metasomatism by ephemeral carbonatite melts. *Nature* **336,** 459–462.

Hauri, E. H., Shimizu, N., Dieu, J. J. & Hart, S. R. (1993). Evidence for hotspot-related carbonatite metasomatism in the oceanic upper mantle. *Nature* **365,** 221–227.

Holness, M. B. (1997). Surface chemical controls on pore fluid connectivity in texturally equilibrated materials. In: Jamveit, B. & Yardley, B. (ed.) *Fluid Flow and Transport in Rocks: Mechanisms and Effects*. London: Chapman and Hall, pp. 149–169.

Hunter, R. H. & McKenzie, D. (1989). The equilibrium geometry of carbonate melts in rocks of mantle composition. *Earth and Planetary Science Letters* **92,** 347–356.

Jones, J. H., Walker, D., Pickett, D. A., Murrell, M. T. & Beattie, P. (1995). Experimental investigations of the partitioning of Nb, Mo, Ba, Ce, Pb, Ra, Th, Pa, and U between immiscible carbonate and silicate liquids. *Geochimica et Cosmochimica Acta* **59,** 1307–1320.

Kjarsgaard, B. & Peterson, T. (1991). Nephelinite–carbonatite liquid immiscibility at Shombole volcano, East Africa—petrographic and experimental evidence. *Mineralogy and Petrology* **43,** 293–314.

Kjarsgaard, B. A., Hamilton, D. L. & Peterson, T. D. (1995). Peralkaline nephelinite/carbonatite liquid immiscibility: comparison of phase compositions in experiments and natural lavas from Oldoinyo Lengai. In: Bell, K. & Keller, J. (ed.) *Carbonatite Volcanism: Oldoinyo Lengai and the Petrogenesis of Natrocarbonatites IAVCEI Proceedings in Volcanology 4*. Berlin: Springer-Verlag, pp. 163–190.

Kogarko, L. (1997). Role of CO_2 on differentiation of ultramafic alkaline series: liquid immiscibility in carbonate-bearing phonolitic dykes (Polar Siberia). *Mineralogical Magazine* **61,** 549–556.

Kushiro, I. (1976). A new furnace assembly with a small temperature gradient in solid-media, high-pressure apparatus. *Carnegie Institution of Washington, Yearbook* **75,** 832–833.

Lee, W.-J. & Wyllie, P. J. (1997*a*). Liquid immiscibility in the join $NaAlSiO_4$–$NaAlSi_3O_8$–$CaCO_3$ at 1 GPa: implications for crustal carbonatites. *Journal of Petrology* **38,** 1113–1135.

Lee, W. J. & Wyllie, P. J. (1997*b*). Liquid immiscibility between nephelinite and carbonatite from 1·0 to 2·5 GPa compared with

mantle melt compositions. *Contributions to Mineralogy and Petrology* **127,** 1–16.

Lee, W. & Wyllie, P. (1998). Petrogenesis of carbonatite magmas from mantle to crust, constrained by the system CaO–(MgO + FeO*)–(Na_2O + K_2O)–(SiO_2 + Al_2O_3 + TiO_2)–CO_2. *Journal of Petrology* **39,** 495–517.

Lee, W. J., Wyllie, P. J. & Rossman, G. R. (1994). CO_2-rich glass, round calcite crystals, and no liquid immiscibility in the system CaO–SiO_2–CO_2 at 2·5 GPa. *American Mineralogist* **79,** 1135–1144.

MacDonald, R., Kjarsgaard, B. A., Skilling, I. P., Davies, G. R., Hamilton, D. I. & Black, S. (1993). Liquid immiscibility between trachyte and carbonate in ash flow tuffs from Kenya. *Contributions to Mineralogy and Petrology* **114,** 276–287.

McKenzie, D. (1985). The extraction of magma from the crust and mantle. *Earth and Planetary Science Letters* **74,** 81–91.

Minarik, W. G. & Watson, E. B. (1995). Interconnectivity of carbonate melt at low melt fraction. *Earth and Planetary Science Letters* **133,** 423–437.

Pyle, J. M. & Haggerty, S. E. (1994). Silicate–carbonate liquid immiscibility in upper-mantle eclogites—implications for natrosilicic and carbonatitic conjugate melts. *Geochimica et Cosmochimica Acta* **58,** 2997–3011.

Rudnick, R. L., McDonough, W. F. & Chappell, B. W. (1993). Carbonatite metasomatism in the northern Tanzanian mantle—petrographic and geochemical characteristics. *Earth and Planetary Science Letters* **114,** 463–475.

Stoppa, F. & Woolley, A. (1997). The Italian carbonatites: field occurrence, petrology and regional significance. *Mineralogy and Petrology* **59,** 43–67.

Wanamaker, B. J. & Kohlstedt, D. L. (1991). The effect of melt composition on the wetting angle between silicate melts and olivine. *Physics and Chemistry of Minerals* **18,** 26–36.

Watson, E. B. (1991). Diffusion in fluid-bearing and slightly-melted rocks—experimental and numerical approaches illustrated by iron transport in dunite. *Contributions to Mineralogy and Petrology* **107,** 417–434.

Watson, E. B. & Lupulescu, A. (1993). Aqueous fluid connectivity and chemical transport in clinopyroxene-rich rocks. *Earth and Planetary Science Letters* **117,** 279–294.

Watson, E. B., Brenan, J. M. & Baker, D. R. (1990). Distribution of fluids in the continental lithospheric mantle. In: Menzies, M. A. (ed.) *Continental Mantle*. Oxford: Clarendon Press, pp. 111–125.

Wolff, J. A. (1994). Physical properties of carbonatite magmas inferred from molten salt data, and application to extraction patterns from carbonatite silicate magma chambers. *Geological Magazine* **131,** 145–153.

Yaxley, G. M. & Green, D. H. (1996). Experimental reconstruction of sodic dolomitic carbonatite melts from metasomatised lithosphere. *Contributions to Mineralogy and Petrology* **124,** 359–369.